PERGAMON

Solid State Communications 119 (2001) 7–12

solid state communications

www.elsevier.com/locate/ssc

Ferroelectric domain structures in PZN–8%PT single crystals studied by scanning force microscopy

M. Abplanalp[a], D. Barošová[b,*], P. Bridenbaugh[c], J. Erhart[b,d], J. Fousek[b,d], P. Günter[a], J. Nosek[d], M. Šulc[b]

[a]*Nonlinear Optics Laboratory, Institute of Quantum Electronics, ETH Hőnggerberg, CH-8093 Zürich, Switzerland*
[b]*Department of Physics, Technical University of Liberec, CZ-46117 Liberec, Czech Republic*
[c]*Crystal Associates, Inc., 31 Farinella Drive, East Hanover, NJ 07936, USA*
[d]*International Center for Piezoelectric Research, Technical University of Liberec, CZ-46117 Liberec, Czech Republic*

Received 23 March 2001; accepted 1 May 2001 by P. Wachter

Abstract

Domain structures in unpoled PZN–8%PT single-crystal (001) plates have been investigated by scanning force microscopy in the piezoresponse mode, at room temperature. Regular fingerprint structure of nonferroelastic domains with antiparallel polarization (of typical width 1–2 μm) has been observed. Compared to domain patterns usually observed in other materials, domains are rather diffuse, with irregular domain walls. The latter are preferably oriented parallel to {211}- or {231}-type planes. Antiparallel polarization switching induced by local application of electric field was clearly demonstrated. Probable ferroelastic (110) domain walls have been also identified and corresponding domain structures have been analyzed.

PACS: 77.80.Dj; 77.84.Dy; 77.65.−j

Keywords: A. Ferroelectrics; C. Scanning force microscopy; D. Piezoelectricity, electrostriction

1. Introduction

Solid solutions of $Pb(Zn_{1/3}Nb_{2/3})O_3$ (PZN) and $PbTiO_3$ (PT) were investigated for the first time by Kuwata et al. [1]. PZN and PT are relaxor and normal ferroelectrics with rhombohedral (3*m*) and tetragonal (4*mm*) symmetry at room temperature, respectively. Their solid solutions (PZN–PT) exist in a wide concentration range of PT content. The PZN–PT system has a morphotropic phase boundary (MPB) [1] at 8–10%PT volume content in the range of technically applicable temperatures. Due to the special poling procedure, PZN–PT could reach hysteresis-free strain vs. electric field dependence, with high strain values (up to 1%) and extremely strong piezoelectric properties ($d_{33} = 2000$ pC/N and $k_{33} = 90\%$) [2–4]. Such superior material characteristics arise as a consequence of the domain engineered crystal structure. Due to such material properties, the PZN–PT domain engineered crystals are promising candidates for further applications [5,6]. Recent symmetry analysis [7] showed that in this and other crystalline ferroic materials multidomain systems could be formed with different symmetries offering new averaged macroscopic properties.

Macroscopic properties of this material have been studied extensively during the last decade [2–4] by various methods (resonant, ultrasound etc.). Observations of the domain structure and its static and dynamic behavior have been investigated at different temperatures and under various conditions of applied electric field [8–12]. Recently, surface morphology has been also observed by scanning force microscopy (SFM) [13]. However, no observations in the piezoresponse SFM mode on the PZN–PT single-crystals have been reported up to now. Using this method, ferroelectric domains can be distinguished on the basis of different piezoelectric response in the directions normal and parallel to the sample surface scanned by the SFM tip.

* Corresponding author. Tel.: +420-48-535-3489; fax: +420-48-510-5882.

E-mail address: dagmar.barosova@vslib.cz (D. Barošová).

0038-1098/01/$ - see front matter
PII: S0038-1098(01)00201-0

Table 1
Components of the piezoelectric coefficient parallel and perpendicular to the crystal surface for permissible domain states in the rhombohedral ferroelectric phase. Contrast of the measured response in the piezoresponse mode SFM corresponds to the listed components

	$d_{\perp}$	$d_{\parallel 1}$	$d_{\parallel 2}$
P^{I}	$+d_{11}^{\mathrm{eff}}$	$+d_{15}^{\mathrm{eff}}$	$+d_{15}^{\mathrm{eff}}$
P^{II}	$+d_{11}^{\mathrm{eff}}$	$-d_{15}^{\mathrm{eff}}$	$+d_{15}^{\mathrm{eff}}$
P^{III}	$+d_{11}^{\mathrm{eff}}$	$-d_{15}^{\mathrm{eff}}$	$-d_{15}^{\mathrm{eff}}$
P^{IV}	$+d_{11}^{\mathrm{eff}}$	$+d_{15}^{\mathrm{eff}}$	$-d_{15}^{\mathrm{eff}}$
P^{V}	$-d_{11}^{\mathrm{eff}}$	$-d_{15}^{\mathrm{eff}}$	$-d_{15}^{\mathrm{eff}}$
P^{VI}	$-d_{11}^{\mathrm{eff}}$	$+d_{15}^{\mathrm{eff}}$	$-d_{15}^{\mathrm{eff}}$
P^{VII}	$-d_{11}^{\mathrm{eff}}$	$+d_{15}^{\mathrm{eff}}$	$+d_{15}^{\mathrm{eff}}$
P^{VIII}	$-d_{11}^{\mathrm{eff}}$	$-d_{15}^{\mathrm{eff}}$	$+d_{15}^{\mathrm{eff}}$

Piezoresponse mode SFM observations have been reported recently, e.g. on $PbTiO_3$ [14], $BaTiO_3$ [15,16] and on TGS [16].

The main aim of the present work is to visualize domain structures in unpoled PZN–8% PT single-crystal, in particular domains with antiparallel polarization, which could not be distinguished optically. A crystal plate with major faces of (001) orientation has been studied; such samples, when poled, exhibit the strongest piezoelectric response.

2. Experimental method

PZN–PT single-crystals were provided by Crystal Associates, Inc., East Hanover, NJ, USA. Crystals of $Pb(Zn_{1/3}Nb_{2/3})O_3$–$PbTiO_3$ (PZN–PT) were grown by method of spontaneous nucleation and slow cooling. In this method, the solution in this case PbO flux and PZN–PT are heated until the entire solution is molten and then cooled through the saturation temperature to create nuclei that grow as the solution is cooled further. Many crystals of varying size are grown by this method. The amount of PT in the solid solution is always very close to that in the starting mixture.

PZN–8%PT has a chemical composition that corresponds to rhombohedral ferroelectric phase close to the MPB at room temperature. Square plates ($5 \times 5 \times 0.68\ \mathrm{mm}^3$) used in this work were oriented with their major faces parallel to a cubic (001) plane. The samples were polished to the surface quality allowing for optical microscopy observations. One of the main crystal faces was electroded by silver paste and glued to the SFM holder. The opposite crystal surface without electrode was subjected to SFM tip scanning.

The SFM images were obtained in the piezoresponse mode using commercially available equipment (Topometrix). All scans were performed at room temperature with a doped silicon SFM tip. In this method, the tip is in firm contact with the sample surface. An ac voltage

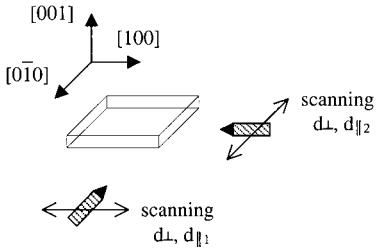

Fig. 1. Sample geometry with the scanning tip directions and the piezoelectric coefficients detectable by SFM.

$U(t) = U_0 \sin(\omega t)$ is applied between the conducting tip and the counter electrode to induce polarization-dependent sinusoidal vibrations of the ferroelectric sample due to the inverse piezoelectric effect. The frequency of the ac voltage was 20 kHz. An electronic feedback is used to keep the dc force on the cantilever constant. The resulting perpendicular cantilever vibration represents the normal component ($d_{\perp}$) of piezoelectric coefficient, while lateral vibrations yield components parallel ($d_{\parallel 1}$ or $d_{\parallel 2}$) to the surface (see Table 1 and Fig. 1). Normal as well as parallel components of the piezoelectric response can be expressed, using basic crystallographic rhombohedral piezoelectric coefficients d_{31}, d_{33}, d_{15}, d_{22}, as

$$d_{11}^{\mathrm{eff}} = \frac{2}{3\sqrt{3}} d_{15} - \frac{4}{3\sqrt{6}} d_{22} + \frac{2}{3\sqrt{3}} d_{31} + \frac{1}{3\sqrt{3}} d_{33} \tag{1a}$$

$$d_{15}^{\mathrm{eff}} = \frac{1}{3\sqrt{3}} d_{15} + \frac{4}{3\sqrt{6}} d_{22} - \frac{2}{3\sqrt{3}} d_{31} + \frac{2}{3\sqrt{3}} d_{33}. \tag{1b}$$

Simultaneously, the sample surface topography is recorded so that any influence of the surface morphology can be analyzed.

3. Results and discussion

Rhombohedral ferroelectric phase allows for the existence of eight domain states with spontaneous polarization vectors oriented in the directions of cube diagonals of the parent cubic phase, i.e.

$$P^{\mathrm{I}} = \frac{1}{\sqrt{3}} P_{\mathrm{S}}(111),\ P^{\mathrm{II}} = \frac{1}{\sqrt{3}} P_{\mathrm{S}}(1\bar{1}1),$$
$$P^{\mathrm{III}} = \frac{1}{\sqrt{3}} P_{\mathrm{S}}(\bar{1}\bar{1}1),\ P^{\mathrm{IV}} = \frac{1}{\sqrt{3}} P_{\mathrm{S}}(\bar{1}11), \tag{2a}$$

$$P^{\mathrm{V}} = \frac{1}{\sqrt{3}} P_{\mathrm{S}}(\bar{1}\bar{1}\bar{1}),\ P^{\mathrm{VI}} = \frac{1}{\sqrt{3}} P_{\mathrm{S}}(\bar{1}1\bar{1}),$$
$$P^{\mathrm{VII}} = \frac{1}{\sqrt{3}} P_{\mathrm{S}}(11\bar{1}),\ P^{\mathrm{VIII}} = \frac{1}{\sqrt{3}} P_{\mathrm{S}}(1\bar{1}\bar{1}). \tag{2b}$$

Domain structure has been observed by the piezoresponse mode SFM in an (001) cut of unpoled PZN–8%PT single-crystal. Typically, fingerprint patterns have been

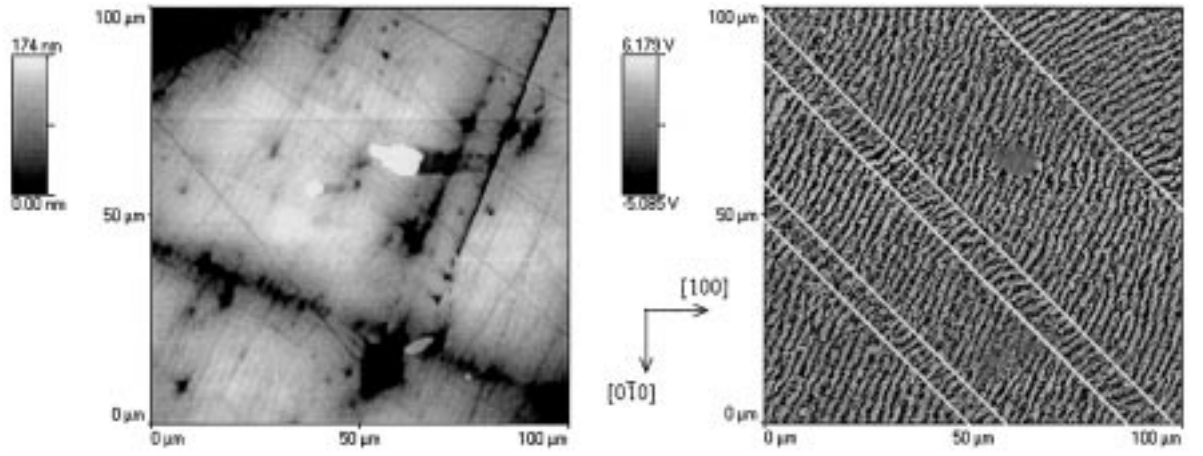

Fig. 2. Piezoresponse mode SFM scan on PZN–8%PT (001) crystal. Added white diagonal lines correspond to the preferred orientation of the ferroelastic (110) domain walls. Topography (left) and normal piezoelectric response (right) is displayed.

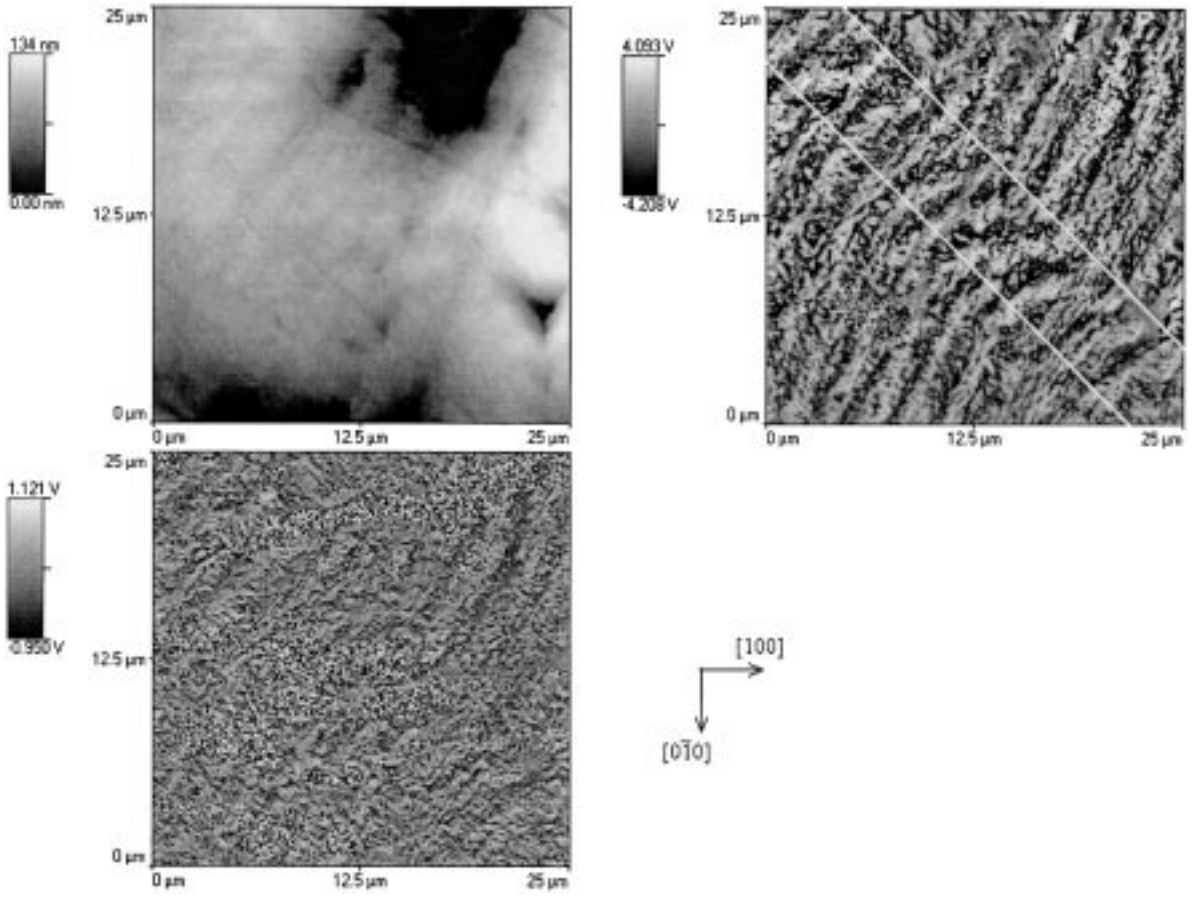

Fig. 3. Piezoresponse mode SFM scan of the domain details. Added white diagonal lines correspond to the preferred orientation of the ferroelastic (110) domain walls. Topography (upper left), normal (upper right) and in-plane (lower left) piezoelectric response is displayed.

Table 2
Permissible domain wall orientations in $m\bar{3}m \rightarrow 3m$ ferroelectrics

	P^{I}	P^{II}	P^{III}	P^{IV}	P^{V}	P^{VI}	P^{VII}	P^{VIII}
P^{I}	N/A	(010) (101)	(001) (110)	(100) (011)	Any	(010) (101)	(001) (110)	(100) (011)
P^{II}		N/A	(100) (0–11)	(001) (−110)	(010) (101)	Any	(100) (0–11)	(001) (−110)
P^{III}			N/A	(010) (−101)	(001) (110)	(100) (0–11)	Any	(010) (−101)
P^{IV}				N/A	(100) (011)	(001) (−110)	(010) (−101)	Any
P^{V}					N/A	(010) (101)	(001) (110)	(100) (011)
P^{VI}						N/A	(100) (0–11)	(001) (−110)
P^{VII}							N/A	(010) (−101)
P^{VIII}								N/A

observed such as shown in Fig. 2. In the SFM picture corresponding to the normal piezoelectric component, parallel stripes appear with a pronounced contrast. While the domain contours are not as clear as in normal ferroelectrics like $BaTiO_3$, these fingerprint patterns can be without any doubt interpreted as domains with antiparallel polarization. Domain wall contours appear very diffuse and irregular, however, with preferred domain wall orientation. Also the domain regions do not represent uniform domains but appear to be composed from the mixture of small regions of both antiparallel domains (see detail in Fig. 3). Regions with different preferred domain wall orientations are in contact at the interfaces whose orientation is close to (110) planes. This plane is the permissible domain wall [17] between certain ferroelectric–ferroelastic domain states, e.g. P^{I} and P^{V}, or P^{III} and P^{VII} (see Table 2). Black and white stripes corresponding to antiparallel domains

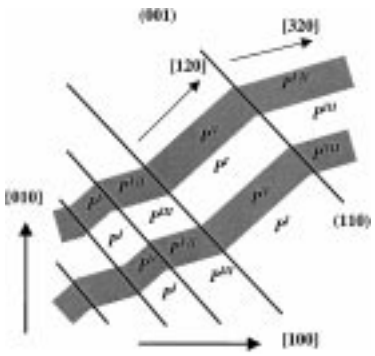

Fig. 4. Suggested domain spatial distribution for unpoled PZN–8%PT (001) single-crystal as observed by SFM.

interpenetrate the probable (110) ferroelastic domain walls continuously.

Analysis of possible spatial distribution of domains in the observed crystal sample suggests the domain configuration as it is shown in Fig. 4. Information about the domain wall orientation and possible SFM contrast (Table 1) in the figure corresponding to normal piezoelectric component is used to analyze Fig. 4. Unfortunately, contrast in the picture of the SFM piezoelectric component parallel to the crystal (001) surface (not shown in Fig. 2) is very weak and a lot of noise is observed. This piezoelectric component usually shows very poor contrast in all scans and gives usually no information because of the noise.

Typical width of antiparallel domains, as analyzed from the SFM pictures, amounts to 1–2 μm. In contrast, the width of the ferroelastic domain is about one order of magnitude larger (about 10 μm). In optical observations (Fig. 5), ferroelastic domain structure has been visualized with typical domain thickness of 150–200 μm. Ferroelastic domain walls cover macroscopic regions in the crystal whose length is typically several mm. It appears that the domain structure is complicated, with several typical dimension levels. The SFM method is very sensitive and covers only the region of 100×100 μm in one scan. Basically, it is not possible to find exactly the same spot observed by the optical microscope and by SFM.

As it is seen in Fig. 2, the energy connected with antiparallel domains prefers certain crystallographic directions of the latter. Projections of antiparallel domain walls (also called 180°-domain walls) on the (001) crystal surface are close to the crystallographic [320] and [120] directions. It is known that 180° walls are preferably oriented parallel to the spontaneous polarization vector, to avoid the existence of

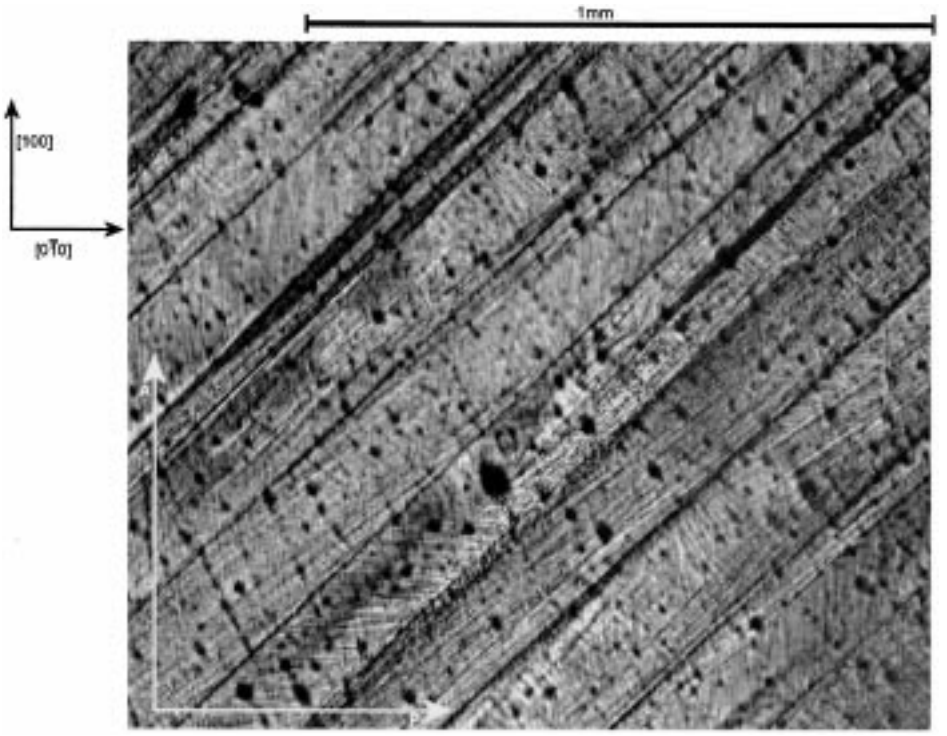

Fig. 5. Optical microscopy on unpoled PZN–8%PT crystal oriented in (001) direction.

bound charge. Thus the energetically preferred domain wall orientation could be calculated as a vector product of the spontaneous polarization vector and a projection of the domain wall on the crystal surface, i.e. {211}- or {231}-type planes for the domain pairs P^{I} and P^{V}, or P^{III} and P^{VII} (Fig. 4).

While there is no doubt that the contrast is due to antiparallel domains, the domain pattern itself is very different from that in classical ferroelectrics like $BaTiO_3$ or TGS, where antiparallel domains have clearly specified and bound geometries. However, it will be the subject of further investigations to clarify whether the observed pattern is connected with some aberrations in the crystal lattice itself or if it is due to chaotical distribution of defects.

In addition to passive observations, the SFM method in the contact mode offers another very useful investigative tool, namely a locally induced switching process. If a dc voltage is applied to the tip, the sample could be locally poled and this will be analyzed in subsequent SFM scans. This offers an easy way to check whether the observed pattern really corresponds to ferroelectric domains. Using such technique with dc voltage of ± 30 V applied to the SFM tip, we have succeeded in 'writing' domains: positive and negative contrast regions were created on the crystal surface. Fig. 6 shows a white and a black region corresponding to $+30$ and -30 V at the tip, respectively. Changes in the domain pattern due to poling clearly demonstrate that the observed pattern really represents ferroelectric domains. In addition, the poling process may not have penetrated deeper in the sample than as detected by the tip. These are probably the reasons why even in the poled regions we can see some remnants of the previous antiparallel domain structure also.

4. Conclusions

The domain structure of unpoled PZN–8%PT single-crystal has been analyzed by scanning force microscopy in the piezoresponse mode. Regular fingerprint structure of antiparallel ferroelectric domains has been observed on the (001) crystal plate. Typical width of these domains is 1–2 μm. Energetically favorable domain wall orientations belong to {211}- and {231}-type of crystallographic planes. In addition, probable ferroelastic (110) domain walls have been identified. Typical width of ferroelastic domains is one order of magnitude larger (about 10 μm). Optically observed ferroelastic domains whose typical width is 150–200 μm have not been recognized clearly in the SFM observations. Ferroelectric nature of the observed pattern has been checked by the poling experiment. Antiparallel domains are clearly influenced by the dc voltage applied to the crystal and a new domain structure is created.

Spatial distribution of domains in PZN–8%PT single-crystal is complicated. The antiparallel domains are rather diffuse with irregular domain walls as compared to the

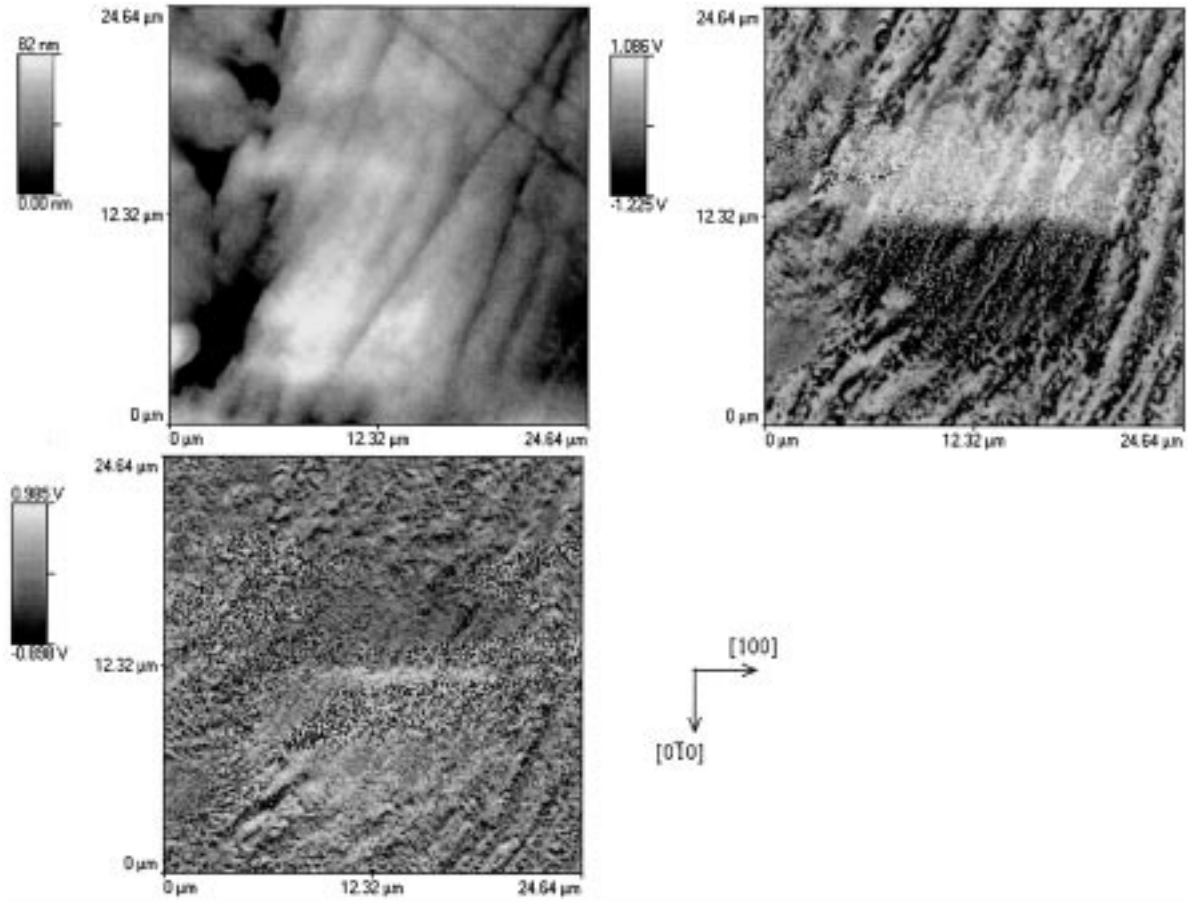

Fig. 6. Poling experiment using SFM tip on (001) PZN–8%PT crystal surface. Black and white regions correspond to −30 and +30 V applied to the SFM tip. Topography (upper left), normal (upper right) and in-plane (lower left) piezoelectric response is displayed.

well-defined regions separated by well-defined domain walls much narrower than domain themselves, as usually observed in other materials. Several domain structures of different size levels exist in the unpoled PZN–PT crystal.

Acknowledgements

This work has been sponsored by DARPA and the Swiss National Science Foundation.

References

[1] J. Kuwata, K. Uchino, S. Nomura, Jpn. J. Appl. Phys. 21 (1982) 1298.
[2] S.E. Park, T.R. Shrout, IEEE Trans. UFFC 44 (1997) 1140.
[3] S.E. Park, T.R. Shrout, J. Appl. Phys. 82 (1997) 1804.
[4] J. Yin, B. Jiang, W. Cao, IEEE Trans. UFFC 47 (2000) 285.
[5] S. Saitoh, T. Kobayashi, K. Harada, S. Shimanuki, Y. Yamashita, IEEE Trans. UFFC 45 (1998) 1071.
[6] S. Saitoh, T. Kobayashi, K. Harada, S. Shimanuki, Y. Yamashita, IEEE Trans. UFFC 46 (1999) 152.
[7] J. Fousek, D.B. Litvin, L.E. Cross, J. Phys. Condens. Matter 13 (2001) 33.
[8] U. Belegundu, X.H. Du, L.E. Cross, K. Uchino, Ferroelectrics 221 (1999) 67.
[9] S. Wada, S.-E. Park, L.E. Cross, T.R. Shrout, Ferroelectrics 221 (1999) 147.
[10] Z.G. Ye, M. Dong, L. Zhang, Ferroelectrics 229 (1999) 223.
[11] J. Yin, W. Cao, J. Appl. Phys. 87 (2000) 7438.
[12] K. Fujishiro, R. Vlokh, Y. Uesu, Y. Yamada, J.-M. Kiat, B. Dkhil, Y. Yamashita, Jpn. J. Appl. Phys. 37 (1998) 5246.
[13] H. Yu, V. Gopalan, J. Sindel, C.A. Randall, J. Appl. Phys. 89 (2001) 561.
[14] P. Lehnen, J. Dec, W. Kleemann, J. Phys. D.: Appl. Phys. 33 (2000) 1932.
[15] L.M. Eng, M. Bammerlin, Ch. Loppacher, M. Guggisberg, R. Bennewitz, R. Lüthi, E. Meyer, Th. Huser, H. Heinzelmann, H.-J. Güntherodt, Ferroelectrics 222 (1999) 153.
[16] M. Abplanalp, L.M. Eng, P. Günter, Appl. Phys. A 66 (1998) 231.
[17] J. Fousek, V. Janovec, J. Appl. Phys. 40 (1969) 135.